doi: 10.4149/gpb_2025029

Transcription factor SPI1 exacerbates the malignant progression of esophageal squamous cell carcinoma byactivating LAMA3 expression

Juan Qin[1,*], Yunxiang Tang[2,*], Rui Zhu[3], Xuqin Feng[1], Jun Bie[1], Qikun Lv[4] and Yang Shu[5]

[1] *Department of Oncology, Beijing Anzhen Nanchong Hospital, Capital Medical University & Nanchong Central Hospital, Nanchong, Sichuan, China*
[2] *Department of Nuclear Medicine, Chongging University Central Hospital, Chongging Emergency Medical Center, Chongqing, China*
[3] *Department of Intensive Care Unit, Beijing Anzhen Nanchong Hospital, Capital Medical University & Nanchong Central Hospital, Nanchong, Sichuan, China*
[4] *Chongqing Key Laboratory of Translational Research for Cancer Metastasis and Individualized Treatment, Chongqing University Cancer Hospital & Chongqing Cancer Institute & Chongqing Cancer Hospital, Chongqing, China*
[5] *Department of Obstetrics and Gynecology, The Second Affiliated Hospital of Chongqing Medical University, Chongqing, China*

Abstract. Esophageal squamous cell carcinoma (ESCC) is the most common subtype of esophageal cancer (ESCA). ESCC is one of the malignancies with high incidence and mortality rates. Studies have found that laminin subunit alpha 3 (LAMA3) functions as an oncogene in a variety of cancers. SPI1 is highly expressed in ESCC, but whether LAMA3 and SPI1 regulate the development of ESCC is still unclear. In this study, bioinformatics analysis tools were used to predict the expression of LAMA3 and SPI1 in ESCA. Subsequently, the levels of mRNA and protein were respectively detected by RT-qPCR and WB. Then, the cell biological behaviors were measured by CCK-8, colony formation, EdU, and tube formation assays. To investigate the *in vivo* effects of LAMA3 knockdown on ESCC, a xenograft tumor model was established, followed by IHC analysis. Additionally, glucose consumption, lactate production, ROS, and Fe^{2+} levels were determined by the corresponding kits. Besides, the interaction of LAMA3 and SPI1 was examined by ChIP and dual luciferase reporter assays. LAMA3 was highly expressed in ESCC and silencing it could curb the viability and proliferation of ESCC cells, tumor growth *in vivo*, tube formation of HUVECs, and induce oxidative stress and ferroptosis of ESCC cells. SPI1 was highly expressed in ESCC and could bind to the promoter of LAMA3 to jointly regulate the progression of ESCC. This study elucidated that SPI1 aggravated ESCC by binding to the promoter of LAMA3, thereby stimulating the growth and proliferation of ESCC cells and suppressing oxidative stress and ferroptosis.

Key words: ESCC — LAMA3 — SPI1 — Oxidative stress — Ferroptosis

* These authors contributed equally to this study.

Electronic supplementary material. The online version of this article (Doi: 10.4149/gpb_2025029) contains Supplementary material.

Correspondence to: Qikun Lv, Chongqing Key Laboratory of Translational Research for Cancer Metastasis and Individualized Treatment, Chongqing University Cancer Hospital & Chongqing Cancer Institute & Chongqing Cancer Hospital, No. 181, Hanyu Road, Shapingba District, Chongqing 400030, China
E-mail:18581473829@163.com

Yang Shu, Department of Obstetrics and Gynecology, the Second Affiliated Hospital of Chongqing Medical University, No.76, Linjiang Road, Yuzhong District, Chongqing 400010, China
E-mail: yangshusy@outlook.com

© The Authors 2025. This is an **open access** article under the terms of the Creative Commons Attribution-NonCommercial 4.0 International License (https://creativecommons.org/licenses/by-nc/4.0/), which permits non-commercial use, distribution, and reproduction in any medium, provided the original work is properly cited.

Introduction

Esophageal cancer (ESCA) is a malignant tumor that arises from the epithelial cells lining the esophagus. It holds the distinction of being the eighth most prevalent cancer and the sixth most fatal cause of cancer-related deaths globally (Sung et al. 2021; Morgan et al. 2022). From a pathological perspective, ESCA is mainly classified into two subtypes: adenocarcinoma and squamous cell carcinoma. Among them, esophageal squamous cell carcinoma (ESCC) occupies a dominant position, with an incidence rate as high as 90% to 95% of all ESCA cases (Smyth et al. 2017). Despite significant advances in the diagnosis and treatment of ESCC in recent years, the prognosis for patients remains poor. Therefore, exploring the pathogenesis of ESCC and identifying effective therapeutic targets holds immense clinical significance.

The laminin family belongs to the category of high molecular weight glycoproteins, with a molecular weight generally ranging from 805 kDa to 850 kDa (Timpl et al. 1979; Aumailley 2013). Serving as a bridge for adhesion between cells and the matrix, laminin effectively regulates cell adhesion and stability through its tight binding to various basement membrane components. Additionally, it can directly or indirectly regulate the growth and differentiation of cells through interactions with other cells (Halper and Kjaer 2014; Yao 2017). Furthermore, laminin possesses the ability to promote cell migration and spreading on the surface of the matrix, thereby actively participating in cellular migration activities. In conjunction with other extracellular matrix proteins, laminin jointly constructs and maintains the structure and function of the basement membrane (Spenlé et al. 2013; Chavda et al. 2022). Laminin exhibits over 12 distinct subtypes, each serving unique functions in the processes of tumor invasion, angiogenesis, and metastasis. The disruption of the harmonious interaction between cells and these laminin subtypes stands as a pivotal characteristic of malignant diseases (Patarroyo et al. 2002). Laminin subunit alpha 3 (LAMA3), also known as E170, LOCS, etc., encodes a protein that is a vital secretory factor within the Laminin family. In recent years, numerous studies have emerged in quick succession, consistently confirming that LAMA3 plays a pivotal role as an oncogene in various types of cancers (Tang et al. 2019; Dai et al. 2024). In the relevant reports by Islam et al. (2023), the high expression of LAMA3 exhibits significant regulatory effects on the proliferation, adhesion, migration, and epithelial-mesenchymal transition (EMT) processes of cholangiocarcinoma cells, thereby accelerating the progression of cholangiocarcinoma. Furthermore, a separate study proposed that METTL3 has the capacity to interact with LAMA3, facilitating its m6A modification and subsequently increasing its expression. This elevation in LAMA3 levels further boosted the malignant progression of oral squamous cell carcinoma (Ning and Mei 2024). However, the current understanding of LAMA3's function in ESCC remains unclear, and there are even fewer studies on this topic.

SPI1 is a gene within the human genome, named for its association with the proviral integration of the Spleen Focus Forming Virus (SFFV). The transcription factor PU.1, encoded by the SPI1 gene, is pivotal in the development of the hematopoietic system and the differentiation of immune cells (Li et al. 2020; Liu X et al. 2023). SPI1 possessed the ability to directly target HK2, thereby modulating the AKT1/mTOR signaling pathway and exacerbating the progression of malignant melanoma (Liu C et al. 2023). Besides, SPI1 has the ability to enhance the transcription of TPX2 and RNF2 to decrease the radiosensitivity exhibited by lung squamous cell carcinoma cells (Yang et al. 2022). More importantly, Luo et al.'s research unveiled SPI1's pivotal role in the progression of ESCC: it facilitated the metastasis of ESCC by elevating the expression level of the CST1 gene and strengthening the interplay between CST1 and MMP2 (Luo et al. 2023). In light of SPI1's crucial role in ESCC, the current study was designed to explore whether SPI1 could similarly impact LAMA3. We undertook a series of meticulously planned *in vivo* and *in vitro* experiments to rigorously test the hypothesis that SPI1 exacerbated the malignant progression of ESCC by activating LAMA3 transcription. This study aimed to offer a robust theoretical foundation for the identification of therapeutic targets in ESCC and further pioneer a novel approach for personalized treatment strategies in this disease.

Materials and Methods

Bioinformatics analysis

This study first analyzed the differential expression of LAMA3 in various diseases through the UALCAN website. Meanwhile, based on sample data from The Cancer Genome Atlas (TCGA), the specific expression of LAMA3 and SPI1 in ESCA sample types and tumor histology were further explored. Subsequently, the GEPIA website was utilized to verify the levels of LAMA3 and SPI1 in ESCA in 182 tumor tissues and 13 normal tissues. Furthermore, a violin plot was employed to illustrate the correlation between SPI1 and the stage of ESCA, based on data from the GEPIA database.

Clinical samples

A total of 101 pairs of tumor tissues and the adjacent noncancerous tissues were collected from surgically resected ESCC patients at Beijing Anzhen Nanchong Hospital. These patients had not undergone any prior treatment before surgery. It was important to mention that all experimental

procedures conducted in this study were approved by the Ethics Committee of Beijing Anzhen Nanchong Hospital, and all patients provided their written informed consents.

Culture and transfection of cell lines

The human normal esophageal epithelial cell line, BAR-T (Chuan Qiu Biotechnology, Shanghai, China), and the ESCA cell line, TE-10 (Chuan Qiu Biotechnology), were cultivated in the high-glucose Dulbecco's Modified Eagle's Medium (DMEM) (Invitrogen, Carlsbad, USA), supplemented with 10% fetal bovine serum (FBS) (Thermo Fisher Scientific, Rockville, MD, USA) and 1% penicillin/streptomycin (P/S) (Invitrogen). With a slight difference from the above culture methods, human ESCC cell line KYSE150 (Cell Bank of Chinese Academy of Sciences, Shanghai, China) needed to be maintained in RPMI 1640 medium (Invitrogen). All three types of cells were cultivated in an adherent manner and maintained in a 37°C incubator with 5% CO_2.

The shRNA sequences specifically targeting LAMA3 and SPI1 were designed and synthesized by GeneChem (Shanghai, China). Non-targeting shRNA (sh-NC) was used as the negative control. Additionally, an empty pcDNA3.1 overexpression vector (vector, Invitrogen) served as a control. To create the LAMA3 overexpression vector (LAMA3), LAMA3 was cloned into the pcDNA3.1 vector. Using Lipofectamine 3000 (Invitrogen), sh-NC, sh-LAMA3, sh-SPI1, vector or LAMA3 was transfected into TE-10 and KYSE150 cells.

Real-time quantitative PCR (RT-qPCR)

Initially, the extraction of total RNA from the cells was necessary, utilizing the Trizol reagent (Thermo Fisher Scientific). Since RNA was highly susceptible to degradation, it was then converted into cDNA using the Transcriptor First Strand cDNA Synthesis Kit (Roche, Vilvoord, Brussel, Belgium) for later use. The gathered cDNA underwent PCR amplification with specific primers (RiBoBio, Guangzhou, China) using the SYBR Green Realtime PCR Master Mix (Toyobo Co., Osaka, Japan). Ultimately, the relative gene expression levels were determined by employing the $2^{-\Delta\Delta Ct}$ method, which utilized β-actin as an internal control for normalization. The specific primer sequences used for the experiments were displayed in Table 1.

Western blot (WB)

To analyze the protein levels in the cells, WB techniques were implemented. Cellular proteins were extracted utilizing a protein extraction kit (Beyotime, Shanghai, China), and their concentrations were quantified through the BCA Protein Assay Kit (Beyotime). Following this, SDS-PAGE was performed to separate the various proteins. The separated proteins on the gel were then meticulously transferred onto PVDF membranes (GE Healthcare, Piscataway, NJ, USA) and promptly blocked with 5% non-fat milk (Beyotime). After 2 h, the membranes were thoroughly washed three times with 1×TBST buffer and were gently agitated on a shaker at 4°C to ensure uniform binding with Anti-LAMA3 antibody (1:1000, Cat: ab151715, Abcam, Cambridge, UK), Anti-SPI1 antibody (1:1000, Cat: ab302623, Abcam), and Anti-beta Actin antibody (1:500, Cat: ab8226, Abcam). The next day, they were washed again with 1×TBST and then incubated with the Goat Anti-Rabbit IgG H&L (HRP) (1:5000, Cat: ab6721, Abcam) and Goat Anti-Mouse IgG H&L (HRP) (1:5000, Cat: ab6789, Abcam) for 2 h at room temperature. Finally, the proteins were visualized using the BeyoECL Plus Kit (Beyotime), and the resulting protein bands were analyzed with ImageJ software.

Cell viability assay

Cell Counting Kit (CCK-8) (Yeasen, Shanghai, China) was applied to analyze the effect of LAMA3 knockdown on ESCC cell viability. In the first step, TE-10 and KYSE150 cells, which had been transfected with sh-NC and sh-LAMA3, were plated into 96-well plates. It was crucial to set the control group (only medium without cells). Following inoculation, at 24, 48, and 72 h, 100 ml of medium from each well was aspirated and replaced with fresh medium containing 10% CCK-8 working solution. The cells were then incubated in the dark for 3 h to allow for complete reaction between the CCK-8 reagent and the cells. Finally, the absorbance value of each well was measured at a wavelength of 450 nm using a microplate reader. Based on these data, the cell viability was calculated.

Colony formation assay

An assay focused on colony formation was employed to investigate the impact of LAMA3 knockdown on the pro-

Table 1. Primer sequences used for RT-qPCR

Name		Primers for PCR (5'–3')
SPI1	F:	GTTACAGGCGTGCAAAATGG
	R:	ATACTCGTGCGTTTGGCGTT
LAMA3	F:	GTTCACAGCAGCAAAGGGTG
	R:	CAATTGCAGGGAACACACCG
xCT	F:	ATCCATGGCCATTGTCACCA
	R:	CCCAGTAGCCGCTCAGAAAA
β-actin	F:	AGGATTCCTATGTGGGCGAC
	R:	ATAGCACAGCCTGGATAGCAA

F, forward; R, reverse.

liferative behavior of ESCC cells. TE-10 and KYSE150 cells transfected with either sh-NC or sh-LAMA3 were plated into 6-well dishes and incubated at 37°C. After a 14-day incubation period, the cells were initially rinsed with PBS. Afterward, they were fixed with methanol (Thermo Fisher Scientific) for 20 min and stained using 0.05% crystal violet (Thermo Fisher Scientific) solution. Following aspiration of the excess stain with PBS, the colonies were enumerated. It should be noted that the clone formation experiments involved in the supplementary experiments required the introduction of the integrin inhibitor GRGDNP, purchased from Macklin (Shanghai, China), and its use concentration on cells was determined to be 50 mM according to the product instructions.

EdU assay

Cell proliferation was assessed using the BeyoClick™ EdU-594 Cell Proliferation Assay Kit (Beyotime), following a straightforward procedure. Initially, cells were plated into 6-well dishes and allowed to culture overnight. They were then exposed to the EdU working solution for 2 h. After fixation (15 min) with 4% polyformaldehyde (Beyotime) and permeabilization (10 min) with 0.3% Triton X-100 (Beyotime), the cells were stained with 594 Click Additive Solution. The nuclei were counterstained with DAPI (Beyotime). Eventually, the number of cells exhibiting red fluorescence was observed and counted under a fluorescence microscope. Similarly, the EdU experiments in the supplementary figure also required the introduction of GRGDNP (Macklin).

Establishment of a xenograft tumor model

Male BALB/c nude mice, aged six weeks, were acquired from Shanghai Laboratory Animal Company (SLAC, Shanghai, China). All *in vivo* experiments were performed in accordance with ethical standards and approved by the Beijing Anzhen Nanchong Hospital Animal Ethics Committee. KYSE150 cells (5×10^6) with stable LAMA3 knockdown or control cells were injected into the back of mice. Tumor size was recorded every 7 days after tumor cell inoculation, and the mice were sacrificed after 35 days to remove the tumors and weigh them.

Immunohistochemistry (IHC) assay

The tumor tissues, once collected, were submerged in a 10% formalin solution for 24 h for fixation. Subsequently, they underwent dehydration and clearing processes using ethanol and xylene, prior to being embedded in paraffin and sectioned into thin slices of 4 mm. After drying in an incubator maintained at 65°C for 2 h, the slices were deparaffinized and hydrated. To ensure antigen recognition by the antibody, high-pressure heat repair was employed to remove any cross-linked substances potentially formed during fixation. Following inactivation and blocking of the sections, the Anti-LAMA3 antibody (Cat: ab321976, Abcam) and Anti-Ki67 antibody (Cat: ab15580, Abcam) were applied dropwise onto the slices and incubated for an hour each. Post-incubation, the sections were thoroughly washed with PBS, and the Horseradish peroxidase (HRP)-conjugated Goat Anti-Rabbit IgG (Cat: ab6721, Abcam) was added dropwise to facilitate binding with the primary antibody. DAB substrate and DAB chromophore in the DAB substrate kit (Cat: ab64238, Abcam) were drip-added to the section at a ratio of 1:20, and incubated at room temperature in the dark for 10 min until positive staining appeared, while DAB could react with hydrogen ions to produce brown precipitate under the catalysis of HRP. Counterstaining with hematoxylin-eosin (Cat: ab245880, Abcam) was performed, and the sections were dehydrated using ethanol and cleared with xylene before being sealed for microscopic examination. This procedure allowed for the subsequent assessment of LAMA3 and Ki-67 expression levels under the microscope.

Wound healing assay

Initially, TE-10 and KYSE150 cells were respectively transfected with sh-NC and sh-LAMA3 constructs. Once the cells achieved optimal growth conditions, they were harvested and plated into 6-well dishes. As the cells adhered to the dish and reached monolayer confluence, a sterile pipette tip was employed to delicately scratch the cell monolayer in a straight line across the well, generating a consistent scratch. Immediately after washing with PBS, a microscopic image was captured as the baseline at time zero. Following 24 h of incubation in the incubator, the cells were photographed again under the microscope, and the wound healing rate was subsequently analyzed.

Tube formation of HUVECs

To investigate the impact of LAMA3-knockdown ESCC cells on tube formation in HUVECs, the HUVECs were initially subjected to a 24-h starvation period. Following this, the Matrigel (BD Biosciences, San Jose, CA, USA) was diluted to a concentration of 10 mg/ml with medium, thoroughly mixed, and dispensed into each well of a 96-well plate. The plate was then incubated at 37°C for 30 min to allow the Matrigel to solidify into a gel-like substrate. Subsequently, HUVECs were seeded and cultured using the conditioned medium collected from TE-10 and KYSE150 cells that had been transfected with sh-NC or sh-LAMA3. After a 48-h incubation period, the treated HUVECs were resuspended

in complete medium and plated onto the Matrigel-coated 96-well plate at a density of 3×10^4 cells *per* well. Following an additional 48 h of incubation, the formation of a vascular network was observed and documented under the microscope.

Determination of indicators related to glycolytic and ferroptosis

Ferroptosis is a well-recognized form of non-apoptotic cell death that is contingent upon the accumulation of intracellular iron. Characteristic features of ferroptosis include heightened levels of lipid peroxidation, increased ROS production, decreased content of the reducing agent glutathione (GSH), and an abnormal accumulation of intracellular ferrous ions (Fe^{2+}). The main function of xCT is to transport cysteine into the cell for GSH synthesis. To assess the cellular level of ROS, the ROS Assay Kit (Yeasen) in conjunction with flow cytometry was chosen for analysis. In parallel, the xCT mRNA levels in cells were assessed by RT-qPCR using the specific primers shown in Table 1. Of course, the amount of Fe^{2+} in the cells was determined by the Ferrous Ion Content Detection Kit (Solarbio, Beijing, China).

Chromatin immunoprecipitation (ChIP) assay

Cells were treated with a 1% formaldehyde solution (Beyotime) to cross-link the DNA and proteins within them. Following 10 min incubation at 37°C, the cross-linking process was halted by the addition of glycine (Beyotime). Subsequently, the cells underwent lysis and sonication procedures, resulting in the production of chromatin fragments ranging in size from 200 to 300 bp. For the purpose of full binding, prewashed Protein A/G beads (Beyotime) were incubated with SPI1 antibody (Cat: ab302623, Abcam) or IgG antibody (Cat: ab172730, Abcam) for 4 h at 4°C. These antibody-bead complexes were then allowed to incubate overnight at 4°C with the chromatin fragments. To reverse the protein-DNA cross-linking, RNase A (Beyotime) and proteinase K (Beyotime) were introduced into the mixture. Finally, after purifying and recovering the DNA, the enrichment of LAMA3 promoter was detected through RT-qPCR reaction.

Dual luciferase reporter assay

The wild-type (WT) and mutant (MUT) sequences of the LAMA3 promoter were cloned into the pGL3-basic vector (Promega, Madison, WI, USA), resulting in the construction of pGL3-basic-LAMA3-WT and pGL3-basic-LAMA3-MUT plasmids. These constructed plasmids were co-transfected into TE-10 and KYSE150 cells along with the internal control plasmid pRL-TK encoding renilla luciferase and sh-NC or sh-SPI1 using Lipofectamine 3000 (Invitrogen). After 2 days, the cells were collected and lysed. Luciferase activity was then measured using the Dual Luciferase Reporter Assay Kit (Promega).

Statistical analysis

For each experiment, three replicate trials were conducted to ensure reliability. The collected data from these trials were statistically analyzed utilizing GraphPad Prism 8.0 software, and the results were presented in a clear format as the mean ± standard deviation (SD). Differences between the two groups of data were analyzed by Student's *t*-test. One-way or two-way ANOVA were used to assess the data among multiple groups. * $p < 0.05$, ** $p < 0.01$, and *** $p < 0.001$ indicate a statistical significance.

Results

LAMA3 was highly expressed in ESCC tumor clinical samples and cells

Through the UALCAN website, the findings indicated that LAMA3 exhibited abnormal expression in 24 diseases, with particularly high expression levels in ESCA (Fig. 1A). When comparing 184 primary tumor samples with 11 normal samples, it was found that the expression level of LAMA3 in the tumor samples was markedly higher than that in the normal samples (Fig. 1B). Compared to 11 normal tissues, the expression level of LAMA3 was higher than in both 89 adenocarcinoma tissues and 95 squamous cell carcinoma tissues (Fig. 1C). Similarly, the GEPIA database analysis also confirmed that LAMA3 was maintained at a high level in ESCA (Fig. 1D). Subsequently, RT-qPCR and WB were respectively performed on the collected clinical samples of ESCC tumors, revealing a significant upregulation of LAMA3 mRNA and protein in tumor tissues compared to these corresponding normal tissues (Fig. 1E,F). And the relationship between LAMA3/SPI1 expression and clinicopathological parameters of 101 ESCC patients is presented in detail in Table 2. High LAMA3 or SPI1 expression was significantly associated with advanced TNM stage and lymph node metastasis. Moreover, TE-10 and KYSE150 cells exhibiting strikingly elevated LAMA3 expression compared to BAR-T cells (Fig. 1G). These findings suggested that LAMA3 was present at higher levels in tumor tissues and cells of ESCC patients.

The malignant proliferation of ESCC cells in vivo and in vitro was suppressed by knockdown of LAMA3

When TE-10 and KYSE150 cells were transfected with sh-LAMA3, the level of LAMA3 protein in the cells was

down-regulated (Fig. 2A). The CCK-8 assay indicated that the viability of TE-10 and KYSE150 cells was repressed when LAMA3 was silenced (Fig. 2B). Analogously, both colony formation and EdU assays validated that the proliferation of TE-10 and KYSE150 cells was hindered upon inhibition of LAMA3 expression (Fig. 2C,D). After that, an mouse ESCC xenograft model was established, elucidating that the injection of KYSE150 cells with LAMA3 knockdown led to nota-

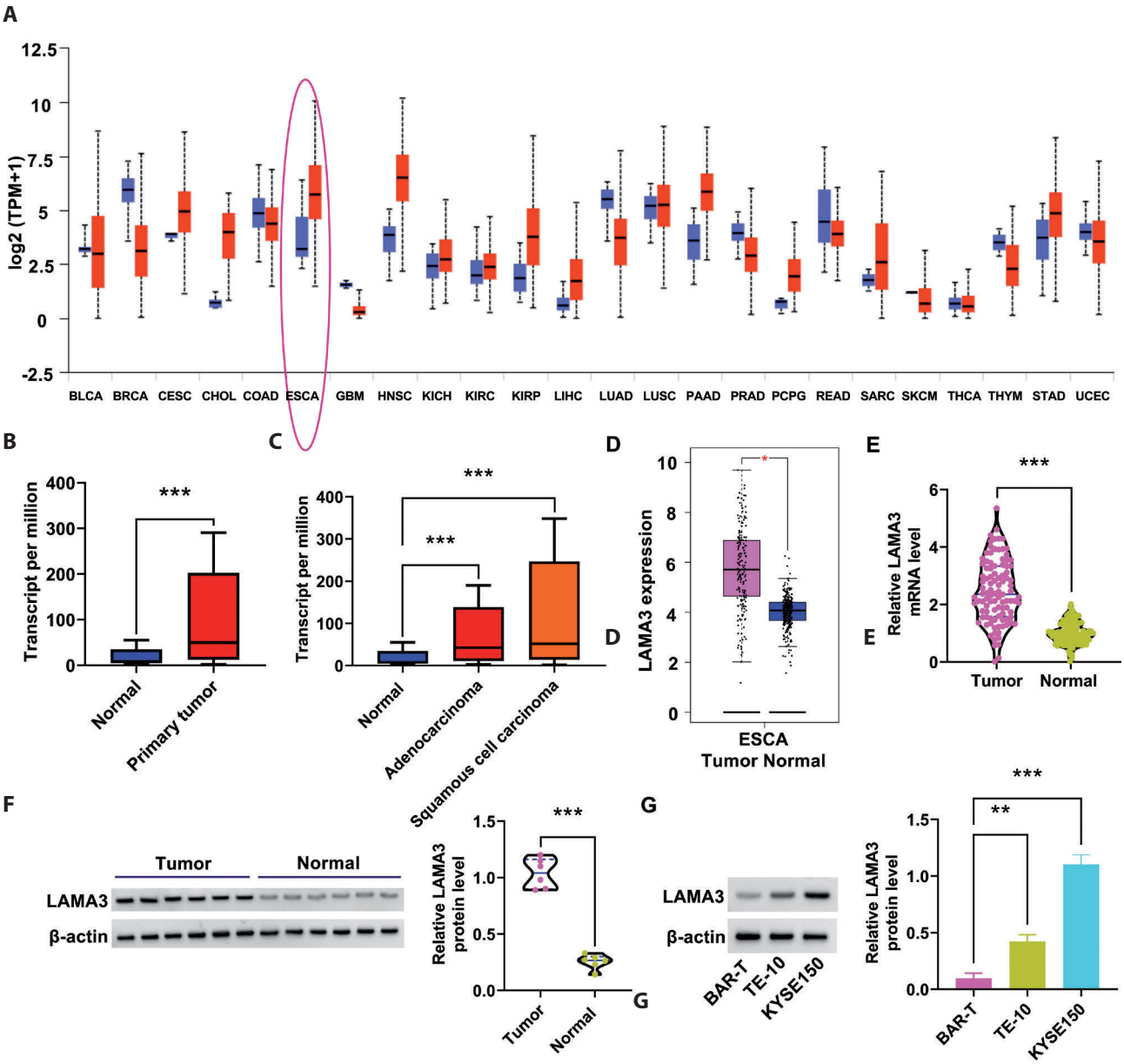

Figure 1. LAMA3 expression in ESCA. **A.** Expression of LAMA3 in different kinds of tumor samples, including ESCA, from the UALCAN database. **B.** The UALCAN database based on The Cancer Genome Atlas (TCGA) samples (Normal: $n = 11$; Primary tumor: $n = 184$) showed LAMA3 expression in ESCA. **C.** LAMA3 expression according to TCGA samples based on tumor histology (Normal: $n = 11$; Adenocarcinoma: $n = 89$; Squamous cell carcinoma: $n = 95$). **D.** The GEPIA website displayed the expression of LAMA3 in ESCA tumor tissues and normal tissues (Tumor: $n = 182$, Normal: $n = 286$). **E.** RT-qPCR was used to detect the expression of LAMA3 mRNA in ESCC tumor tissues and corresponding normal tissues (Tumor: $n = 101$; Normal: $n = 101$). **F.** The level of LAMA3 protein in clinical samples was measured by WB (Tumor: $n = 6$; Normal: $n = 6$). **G.** WB was used to detect the expression of LAMA3 protein in BAR-T, TE-10, and KYSE150 cells. Differences in data were assessed by Student's *t*-test or one-way ANOVA. * $p < 0.05$, ** $p < 0.01$, *** $p < 0.001$.

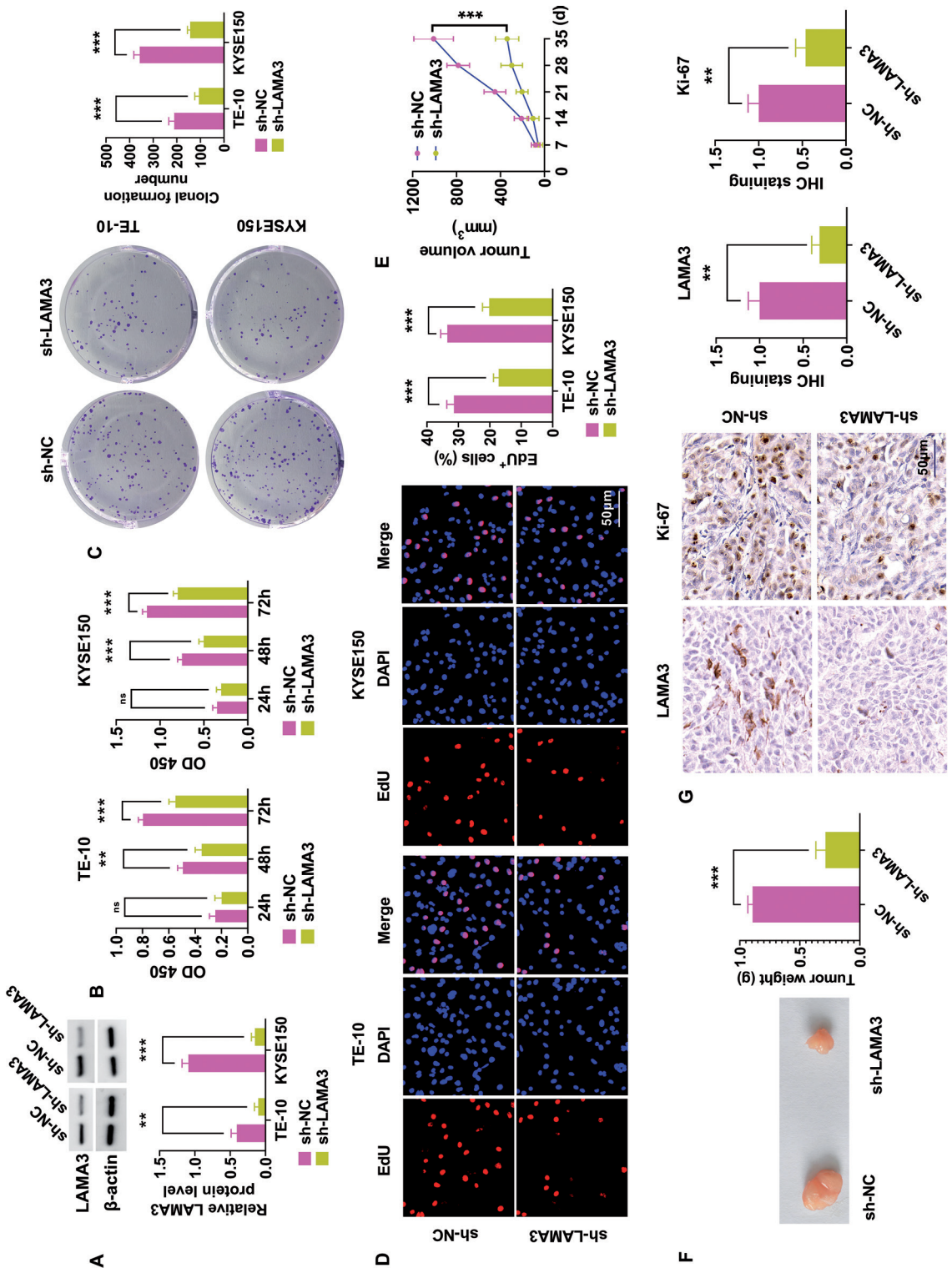

Figure 2. Effect of LAMA3 silencing on the growth and proliferation of ESCC cells *in vitro* and *in vivo*. TE-10 and KYSE150 cells were respectively transfected with sh-NC and sh-LAMA3. **A.** WB analysis of LAMA3 protein level after transfection of sh-NC and sh-LAMA3. **B.** Cell viability was determined by CCK-8 assay. Cell proliferation was monitored by colony formation (**C**) and EdU assays (**D**). KYSE150 cells transfected with sh-NC or sh-LAMA3 were injected subcutaneously into the BALB/c nude mice. **E.** Growth curves of ESCC xenograft tumors. **F.** Images and weights of the removed tumors. **G.** IHC staining was applied to analyze the expression of LAMA3 and Ki-67 in the tumors. Differences in data were assessed by Student's *t*-test, one-way ANOVA, or two-way ANOVA. ** $p < 0.01$, *** $p < 0.001$.

bly slower tumor growth and a reduction in tumor weight in the mice (Fig. 2E,F). The IHC staining results demonstrated a decrease in LAMA3 expression within the tumor tissues of the sh-LAMA3 group, accompanied by a downregulation in the expression of cell proliferation-related gene Ki-67 (Fig. 2G). In summary, the silencing of LAMA3 effectively restrained the viability and proliferation of ESCC cells *in vitro*, as well as tumor growth *in vivo*.

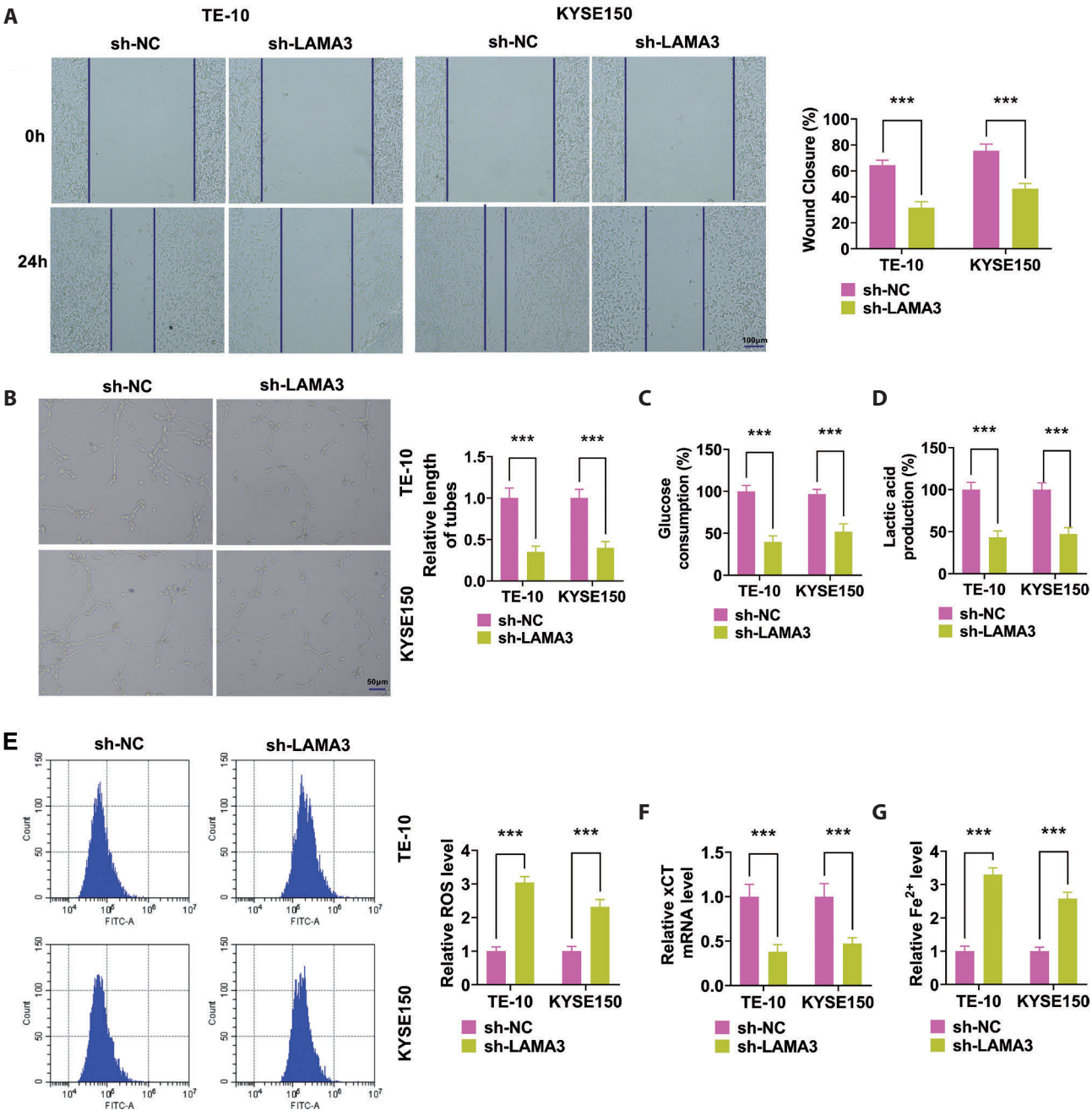

Figure 3. Knockdown of LAMA3 blocked cell migration, angiogenesis, glycolysis, and induced oxidative stress and ferroptosis in ESCC cells. TE-10 and KYSE150 cells were respectively transfected with sh-NC and sh-LAMA3. **A.** Cell migration was examined using wound healing assay. **B.** Tube formation assay was used to detect the tube formation ability of HUVECs. The levels of glucose consumption (**C**) and lactate production (**D**) in TE-10 and KYSE150 cells were measured using corresponding kits. **E.** The corresponding kit was used in combination with flow cytometry to analyze the levels of ROS in TE-10 and KYSE150 cells. **F.** RT-qPCR was utilized to assess the mRNA levels of xCT. **G.** The contents of Fe^{2+} were determined by commercial kits. Differences in data were assessed by Student's *t*-test. *** $p < 0.001$.

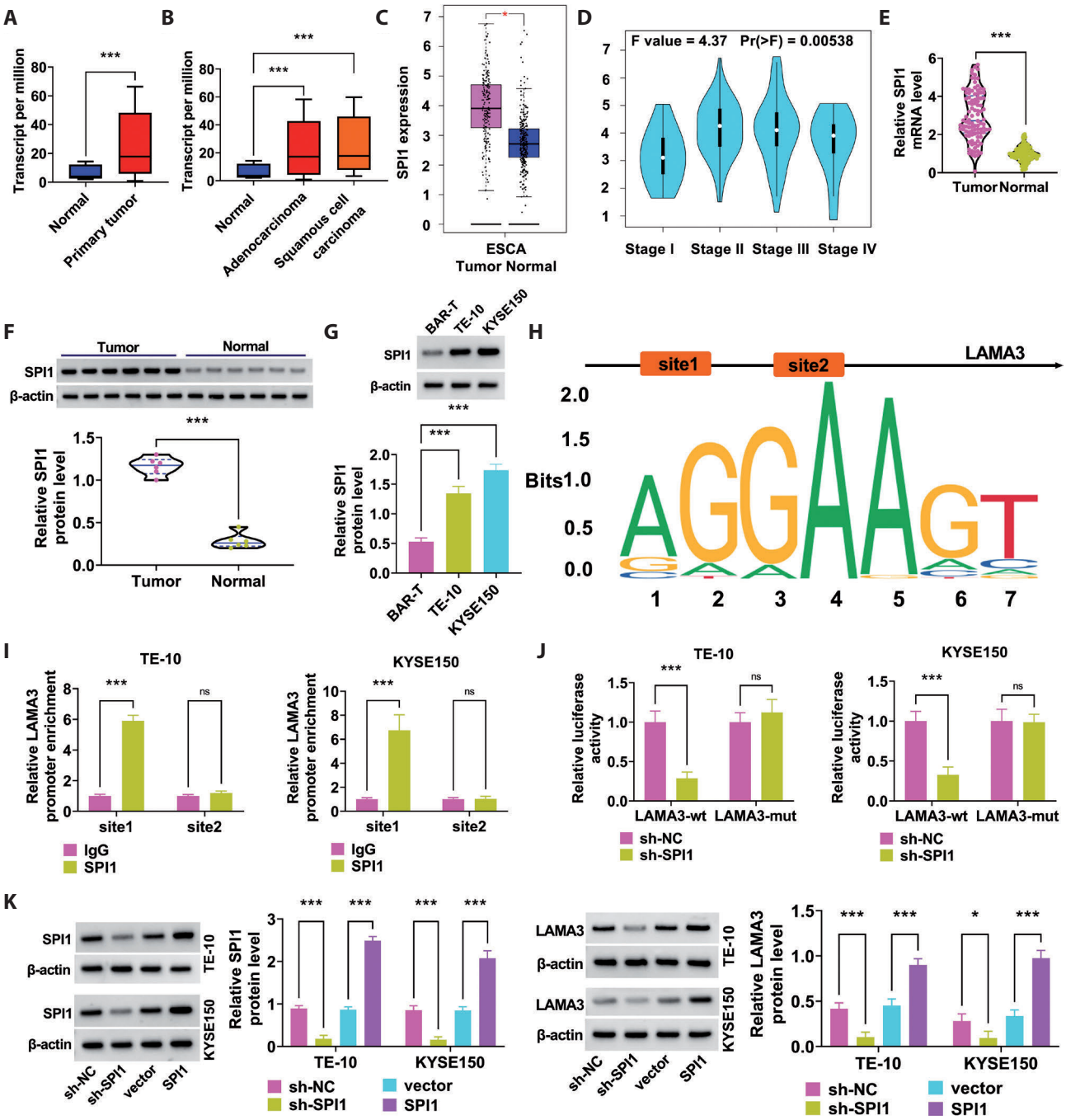

Figure 4. Prediction and validation of the relationship between LAMA3 and SPI1. **A.** The UALCAN database based on TCGA samples (Normal: $n = 11$; Primary tumor: $n = 184$) presented SPI1 expression in ESCA. **B.** SPI1 expression according to TCGA samples based on tumor histology (Normal: $n = 11$; Adenocarcinoma: $n = 89$; Squamous cell carcinoma: $n = 95$). **C.** The GEPIA website showed the expression of SPI1 in ESCA tumor tissues and normal tissues (Tumor: $n = 182$, Normal: $n = 286$). **D.** Expression of SPI1 in ESCA based on cancer stage. **E.** The expression of SPI1 mRNA in ESCC clinical samples was detected by RT-qPCR (Tumor: $n = 101$; Normal: $n = 101$). **F.** WB analysis results of SPI1 protein expression in ESCC clinical samples (Tumor: $n = 6$; Normal: $n = 6$). **G.** WB was employed to detect the expression of SPI1 protein in BAR-T, TE-10, and KYSE150 cells. **H.** The JASPAR website predicts the binding site of SPI1 to the LAMA3 promoter. **I.** The interaction between SPI1 and LAMA3 was analyzed by ChIP. **J.** Their binding between SPI1 and LAMA3 was verified by dual luciferase reporter system. **K.** WB was performed to evaluate the effect of SPI1 knockdown or overexpression on LAMA3 protein expression. Differences in data were assessed by Student's *t*-test, one-way ANOVA, or two-way ANOVA. * $p < 0.05$, *** $p < 0.001$.

Silencing LAMA3 curbed cell migration, angiogenesis, glycolysis, and facilitated oxidative stress and ferroptosis in ESCC cells

As shown in Figure 3A, the wound healing assay revealed a significant inhibition in the migration capability of both TE-10 and KYSE150 cells following transfection with sh-LAMA3. At the same time, the extent of tube formation by HUVECs in the sh-LAMA3 group was also decreased than that in the sh-NC group (Fig. 3B). Likewise, upon inhibition of LAMA3 expression, both TE-10 and KYSE150 cells exhibited a notable decrease in glucose consumption and lactate production (Fig. 3C,D). Then, the kit, in conjunction with flow cytometry, was utilized to confirm a reduction in the level of ROS upon silencing of LAMA3 (Fig. 3E). Additionally, xCT exhibited a decreasing trend, accompanied by an increase in the concentration of Fe^{2+} (Fig. 3F,G). Collectively, the findings implicated that LAMA3 silencing exerted inhibitory effects on tube formation in HUVECs, as well as migration and glycolysis in ESCC cells. Conversely, it activated oxidative stress and ferroptosis pathways in ESCC cells.

SPI1 was highly expressed in ESCC and positively regulated LAMA3

According to the UALCAN and GEPIA database, SPI1 was highly expressed in ESCA primary tumors compared with normal tissues (Fig. 4A–C). And compared to stage I, the expression level of SPI1 is increased in stages II, III, and IV of ESCA (Fig. 4D). Through RT-qPCR and WB analyses of clinical samples from ESCC patients, it was determined that the levels of SPI1 mRNA and protein were elevated in ESCC tumor tissues (Fig. 4E,F). SPI1 protein level was also upregulated in TE-10 and KYSE150 cells (Fig. 4G). Based on the aforementioned results, two SPI1 binding sites were predicted in the promoter region of LAMA3 *via* the JASPAR website (Fig. 4H). ChIP results showed that compared with IgG group, LAMA3 promoter was highly enriched at site 1 in SPI1 antibody group (Fig. 4I). What's more, when SPI1 was knocked down, it significantly attenuated the luciferase activity of WT-LAMA3. However, in the case of promoter site mutation of LAMA3, the knockdown of SPI1 had little impact on its luciferase activity (Fig. 4J). As presented in Fig. 4K, the expression of LAMA3 exhibited synchronous changes with SPI1 levels. The amount of LAMA3 protein decreased when SPI1 was knocked down, and it was increased when SPI1 was overexpressed. To summarize, SPI1 remained abundant in ESCC and was able to bind to the LAMA3 promoter, thereby enhancing LAMA3 levels.

Overexpression of LAMA3 reversed the inhibitory effect of SPI1 knockdown on ESCC cell progression

When TE-10 and KYSE150 cells were transfected with pcDNA3.1-LAMA3, the level of LAMA3 protein was upregulated (Fig. 5A). Given that laminin usually signals through integrins, such as α3β1, α6β4, we introduced the integrin inhibitor GRGDNP to verify whether integrins mediate the tumorpromoting effects of LAMA3. Findings from EdU and wound healing assays demonstrated that GRGDNP effectively suppressed cell proliferation and migration. When GRGDNP existed, the overexpression of LAMA3 failed to enhance the the malignant proliferation and migration of both cell lines (Supplementary material, Fig. S1). This outcome further substantiated that LAMA3 exerted a pro-tumorigenic role *via* integrin signaling. Overexpression of LAMA3 rescued the LAMA3 protein level downregulated by SPI1 knockdown (Fig. 5B). Likewise, sh-SPI1 transfection contributed to a decline in the viability, proliferation, and migration behaviors of TE-10 and KYSE150 cells, yet these behaviors were subsequently ameliorated by overexpressing LAMA3 (Fig. 5C–F). The angiogenesis of HUVECs suppressed by sh-SPI1 was also rescued by LAMA3 overexpression (Fig. 5G). The reduction in glucose consumption and lactate production observed in both TE-10 and KYSE150 cells due to sh-SPI1 transfection was relieved when LAMA3 was overexpressed (Fig. 5H,I). SPI1 knockdown resulted in the increase of ROS and Fe^{2+} levels and the decrease of xCT, but these changes were reversed due to LAMA3 overexpression (Fig. 5J–L). All in all, overexpression of LAMA3 abolished the tumor suppressive effect induced by SPI1 knockdown, suggesting that SPI1/LAMA3 axis jointly aggravated the progression of ESCC.

Discussion

Research has demonstrated that an elevated expression of SIRT1 can bolster the resilience of ESCC to radiotherapy and chemotherapy. This further underscores the potential of SIRT1-targeted therapy as a novel approach to enhancing the therapeutic efficacy of CRT (combining radiotherapy and chemotherapy) for ESCC (Morishita et al. 2024). Similarly, Di et al. (2019) revealed that elevated levels of PLOD2 possess the ability to propel the progression of ESCC through the activation of the FAK/AKT signaling pathway, subsequently accelerating the EMT process. These findings suggest that specific molecules abnormally expressed in ESCC patients hold promise as unique biomarkers for ESCC, and therapeutic strategies that target these biomarkers have the strong potential to pave a novel pathway for the treatment of ESCC.

In this thesis, we focused on the role of LAMA3 in the progression of various diseases and explored whether LAMA3 also contributed to the progression of ESCC. Utilizing the TCGA sample database on the UALCAN website, it was confirmed that LAMA3 exhibited a significantly elevated expression level in primary tumor tissues of ESCA, as compared to normal tissues. Furthermore, a notable observation

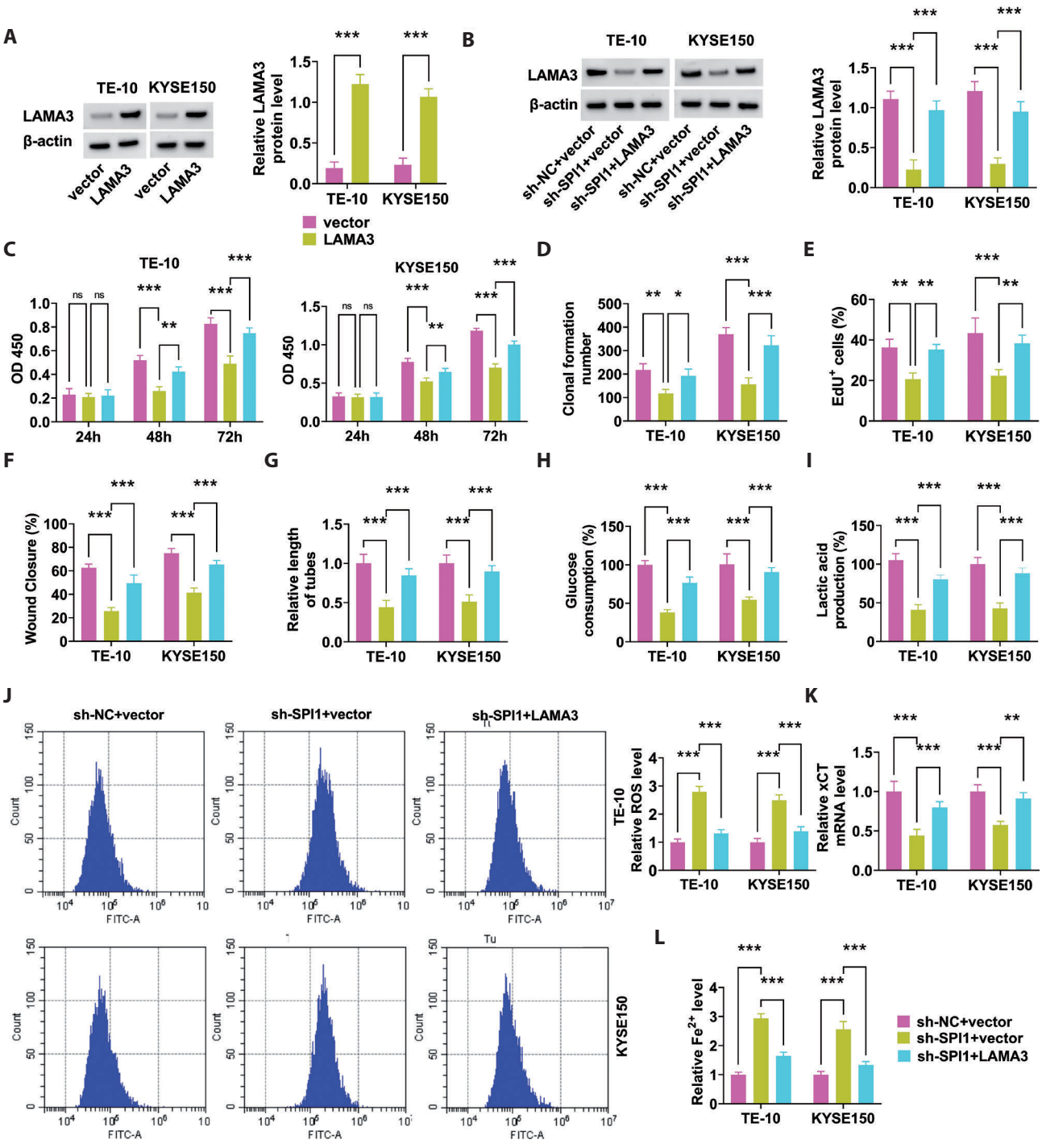

Figure 5. SPI1/LAMA3 regulated the progression of ESCC cells. **A.** The efficiency of LAMA3 overexpression was determined by WB. **B**-**L**.TE-10 and KYSE150 cells were transfected with sh-NC+vector, sh-SPI1+vector, or sh-SPI1+LAMA3. **B.** WB was utilized to analyze the changes of LAMA3 protein levels. **C.** CCK-8 assay was employed to evaluate cell viability. Cell proliferation was measured by colony formation (**D**) and EdU assays (**E**). **F.** Cell migration was analyzed by wound healing assay. **G.** The capacity of HUVECs to form tubes was assessed through a tube formation assay. The glucose consumption (**H**) and lactate production (**I**) were determined by corresponding kits. **J.** The quantification of ROS levels was detected by commercial kit and flow cytometry. **K.** The xCT mRNA levels were evaluated by RT-qPCR. **L.** Levels of Fe^{2+} were analyzed using kits. Differences in data were assessed by Student's *t*-test or one-way ANOVA. * $p < 0.05$, ** $p < 0.01$, *** $p < 0.001$.

was that LAMA3 expression was even higher in ESCC tissues than in adenocarcinoma tissues. Meanwhile, the prediction results given by the GEPIA website are consistent with the above. Therefore, we conducted RT-qPCR and WB analyses on tumor samples and their corresponding adjacent tissues collected from ESCC patients, confirming that the mRNA and protein levels of LAMA3 were markedly elevated in ESCC tumor tissues compared to normal tissues. Additionally, although the level of LAMA3 was also up-regulated in TE-10 cells, the up-regulation trend was more pronounced in KYSE150 cells. This implied that LAMA3 might play a crucial part in the progression of ESCC. Subsequently, LAMA3 underwent a loss-of-function treatment. Knocking down LAMA3 in TE-10 and KYSE150 cells effectively suppressed their growth and proliferation *in vitro*. In the *in vivo* study, the injection of KYSE150 cells featuring LAMA3 knockdown led to a marked decrease in tumor growth rate and a notable reduction in tumor weight, in contrast to the injection of KYSE150 cells without any modification. Furthermore, the gene expression levels of Ki-67, a well-established marker for cancer cell proliferation, were strikingly downregulated in these tumor tissues. Furthermore, our findings revealed that the knockdown of LAMA3 markedly impeded the migration capability of ESCC cells, as evidenced by the wound healing assay. Moreover, the angiogenesis of HUVECs was also hindered. Besides, a reduction in glucose consumption and lactate production served as indicators of impaired metabolism in cancer cells. So, how does LAMA3 induce ESCC cell growth and metastasis? Oxidative stress denotes the disruption of equilibrium between oxidative and antioxidant processes within the body, leading to an overabundance of oxidation and the subsequent production of numerous ROS (Tang et al. 2022). Ferroptosis, on the other hand, emerges as a novel type of iron-dependent programmed cell death, distinguished by a surge in intracellular lipid peroxides and the accumulation of iron ions (Mou et al. 2019; Jiang et al. 2021). On one hand, ROS generated under oxidative stress conditions serve as pivotal mediators in ferroptosis, initiating a chain reaction of lipid peroxidation, a hallmark of this unique cell death process. Conversely, the lipid peroxidation and iron accumulation that occur during ferroptosis exacerbate oxidative stress, thereby perpetuating a vicious cycle (Zeng et al. 2023; Li et al. 2024). Therefore, we initially assessed the levels of ROS and discovered a significant upregulation in ESCC cells that had been transfected with sh-LAMA3. This finding suggested that the knockdown of LAMA3 stimulated oxidative stress in ESCC cells. Concurrently, the mRNA level of xCT was suppressed, while the Fe^{2+} level accumulated in ESCC cells, hinting that the silencing of LAMA3 also triggered ferroptosis. In essence, the overexpression of LAMA3 fueled the proliferation and metastasis of ESCC cells by safeguarding them against oxidative stress and ferroptosis.

To delve deeper into the molecular mechanisms underlying LAMA3's role in ESCC, we directed our focus towards the upstream regulators of LAMA3. The transcription factor SPI1 has been documented to intensify iron accumulation and facilitate the formation of osteoclasts (Liu et al. 2024). Qiu et al. (2023) discovered that SPI1 propelled the progression of gastric cancer by upregulating NMT1, a process facilitated by the PI3K/AKTmTOR signaling pathway. In the pivotal study conducted by Yao et al. (2021), it was unequivocally confirmed that five genes, notably including SPI1, were significantly upregulated in ESCC tumor samples. This upregulation served as a predictive indicator of a poor prognosis in patients with ESCC. Therefore, we formulated the hypothesis that SPI1 and LAMA3 may synergistically collaborate in driving the progression of ESCC. With the help of bioinformatics analysis tools, it was definitively established that SPI1 was also markedly overexpressed in ESCA patients, exhibiting a correlation with the cancer stage. Analogous to LAMA3, SPI1 was abundant in tumor samples obtained from patients and ESCC cells. Moreover, ChIP and dual luciferase reporter assays provided compelling evidence that SPI1 could bind to and interact with the promoter region of LAMA3. Consequently, the protein expression level of LAMA3 was observed to fluctuate in direct response to changes in SPI1 expression. What crucial role does the SPI1/LAMA3 complex play in the progression of ESCC? It was undeniable that when SPI1 was silenced, ESCC cells exhibited the same phenomenon as when LAMA3 was knocked down. In simpler terms, reducing the levels of SPI1 could effectively suppress the growth and dissemination of ESCC cells. However, the anti-tumor effects achieved through SPI1 inhibition were greatly reversed upon overexpression of LAMA3, indicating that SPI1/LAMA3 collaboratively regulated ESCC progression. It was further ascertained that LAMA3 promoted tumor growth and metastasis by through integrin.

Collectively, our findings have unequivocally confirmed the oncogenic role of LAMA3 in ESCC. Moreover, it is demonstrated that SPI1-mediated upregulation of LAMA3 promotes the progression of ESCC by suppressing oxidative stress and ferroptosis within ESCC cells. This underscores the potential of SPI1 and LAMA3 as valuable biomarkers for future advancements in the treatment of ESCC. However, the current application of these results in clinical practice is still insufficient. Therefore, future studies should further explore the intrinsic relationship between SPI1/LAMA3 axis and patient prognosis, tumor stage, and other clinicopathological features.

Data availability statement. Data is available from the corresponding author upon reasonable request.

Conflict of interest. The authors declare that they have no conflict of interest.

References

Aumailley M (2013): The laminin family. Cell. Adh. Migr. **7,** 48-55 https://doi.org/10.4161/cam.22826

Chavda ND, Sari B, Asiri FM, Hamill KJ (2022): Laminin N-terminus (LaNt) proteins, laminins and basement membrane regulation. Biochem. Soc. Trans. **50,** 1541-1553 https://doi.org/10.1042/BST20210240

Dai S, Kong H, Ja Y, Bao L, Wang C, Qin L (2024): Expression of the laminin genes family and its relationship to prognosis in pancreatic carcinoma. Arab. J. Gastroenterol. **25,** 306-314 https://doi.org/10.1016/j.ajg.2024.07.006

Di WY, Kang XH, Zhang JH, Wang Y, Kou WZ, Su W (2019): [Expression of PLOD2 in esophageal squamous cell carcinoma and its correlation with invasion and metastasis]. Zhonghua Bing Li Xue Za Zhi **48,** 102-107 (in Chinese)

Halper J, Kjaer M (2014): Basic components of connective tissues and extracellular matrix: elastin, fibrillin, fibulins, fibrinogen, fibronectin, laminin, tenascins and thrombospondins. Adv. Exp. Med. Biol. **802,** 31-47 https://doi.org/10.1007/978-94-007-7893-1_3

Islam K, Balasubramanian B, Venkatraman S, Thummarati P, Tunganuntarat J, Phueakphud N, Kanjanasirirat P, Khumpanied T, Kongpracha P, Kittirat Y, et al. (2023): Upregulated LAMA3 modulates proliferation, adhesion, migration and epithelial-to-mesenchymal transition of cholangiocarcinoma cells. Sci. Rep. **13,** 22598 https://doi.org/10.1038/s41598-023-48798-8

Jiang X, Stockwell BR, Conrad M (2021): Ferroptosis: mechanisms, biology and role in disease. Nat. Rev. Mol. Cell Biol. **22,** 266-282 https://doi.org/10.1038/s41580-020-00324-8

Li G, Hao W, Hu W (2020): Transcription factor PU.1 and immune cell differentiation (Review). Int. J. Mol. Med. **46,** 1943-1950 https://doi.org/10.3892/ijmm.2020.4763

Li K, Fan C, Chen J, Xu X, Lu C, Shao H, Xi Y (2024): Role of oxidative stress-induced ferroptosis in cancer therapy. J. Cell Mol. Med. **28,** e18399 https://doi.org/10.1111/jcmm.18399

Liu C, Qiu X, Gao J, Gong Z, Zhou X, Luo H, Geng X (2023): SPI1 involvement in malignant melanoma pathogenesis by regulation of HK2 through the AKT1/mTOR pathway. J. Cell Mol. Med. **27,** 2675-2683 https://doi.org/10.1111/jcmm.17844

Liu LL, Liu ZR, Xiao YS, Xiao JH, Huang WM, Liu WY, Zhao K, Ye YJ (2024): SPI1 exacerbates iron accumulation and promotes osteoclast formation through inhibiting the expression of Hepcidin. Mol. Cell Endocrinol. **580,** 112103 https://doi.org/10.1016/j.mce.2023.112103

Liu X, Xu M, Jia W, Duan Y, Ma J, Tai W (2023): PU.1 negatively regulates tumorigenesis in non-small-cell lung cancer. Med. Oncol. **40,** 79 https://doi.org/10.1007/s12032-023-01946-6

Luo FF, Wang J, Zhang ZF, Lin ST, Huang TJ, Liu BQ, Fan ML, Peng LX, Zheng ST, Yang CF, et al. (2023): SPI1-mediated upregulation of the CST1 gene as an independent poor prognostic factor accelerates metastasis in esophageal squamous cell carcinoma (ESCC) by interacting with MMP2. Front. Biosci. (Landmark Ed) **28,** 212 https://doi.org/10.31083/j.fbl2809212

Morgan E, Soerjomataram I, Rumgay H, Coleman HG, Thrift AP, Vignat J, Laversanne M, Ferlay J, Arnold M (2022): The Global landscape of esophageal squamous cell carcinoma and esophageal adenocarcinoma incidence and mortality in 2020 and projections to 2040: New estimates from GLOBOCAN 2020. Gastroenterology **163,** 649-658 https://doi.org/10.1053/j.gastro.2022.05.054

Morishita H, Otsuka R, Murakami K, Endo S, Toyozumi T, Matsumoto Y, Shiraishi T, Iida S, Makiyama T, Nishioka Y, et al. (2024): SIRT1 promotes chemoradiotherapy resistance in esophageal squamous cell carcinoma. Oncology **102,** 960-968 https://doi.org/10.1159/000540247

Mou Y, Wang J, Wu J, He D, Zhang C, Duan C, Li B (2019): Ferroptosis, a new form of cell death: opportunities and challenges in cancer. J. Hematol. Oncol. **12,** 34 https://doi.org/10.1186/s13045-019-0720-y

Ning B, Mei Y (2024): LAMA3 promotes tumorigenesis of oral squamous cell carcinoma by METTL3-mediated N6-methyladenosine modification. Crit. Rev. Immunol. **44,** 49-59 https://doi.org/10.1615/CritRevImmunol.2023051066

Patarroyo M, Tryggvason K, Virtanen I (2002): Laminin isoforms in tumor invasion, angiogenesis and metastasis. Semin. Cancer Biol. **12,** 197-207 https://doi.org/10.1016/S1044-579X(02)00023-8

Qiu P, Li X, Gong M, Wen P, Wen J, Xu L, Wang G (2023): SPI1 mediates N-myristoyltransferase 1 to advance gastric cancer progression via PI3K/AKT/mTOR pathway. Can. J. Gastroenterol. Hepatol. **2023,** 2021515 https://doi.org/10.1155/2023/2021515

Smyth EC, Lagergren J, Fitzgerald RC, Lordick F, Shah MA, Lagergren P, Cunningham D (2017): Oesophageal cancer. Nat. Rev. Dis. Primers **3,** 17048 https://doi.org/10.1038/nrdp.2017.48

Spenlé C, Simon-Assmann P, Orend G, Miner JH (2013): Laminin α5 guides tissue patterning and organogenesis. Cell Adh. Migr. **7,** 90-100 https://doi.org/10.4161/cam.22236

Sung H, Ferlay J, Siegel RL, Laversanne M, Soerjomataram I, Jemal A, Bray F (2021): Global cancer statistics 2020: GLOBOCAN estimates of incidence and mortality worldwide for 36 cancers in 185 countries. CA Cancer J. Clin. **71,** 209-249 https://doi.org/10.3322/caac.21660

Tang L, Wang P, Wang Q, Zhong L (2019): Correlation of LAMA3 with onset and prognosis of ovarian cancer. Oncol. Lett. **18,** 2813-2818 https://doi.org/10.3892/ol.2019.10600

Tang Y, Zhou X, Cao T, Chen E, Li Y, Lei W, Hu Y, He B, Liu S (2022): Endoplasmic reticulum stress and oxidative stress in inflammatory diseases. DNA Cell Biol. **41,** 924-934 https://doi.org/10.1089/dna.2022.0353

Timpl R, Rohde H, Robey PG, Rennard SI, Foidart JM, Martin GR (1979): Laminin--a glycoprotein from basement membranes. J. Biol. Chem. **254,** 9933-9937 https://doi.org/10.1016/S0021-9258(19)83607-4

Yang J, Liu C, Guan J, Wang Y, Su J, Wang Y, Liu S (2022): SPI1 mediates transcriptional activation of TPX2 and RNF2 to regulate the radiosensitivity of lung squamous cell carcinoma. Arch. Biochem. Biophys. **730,** 109425

https://doi.org/10.1016/j.abb.2022.109425
Yao J, Duan L, Huang X, Liu J, Fan X, Xiao Z, Yan R, Liu H, An G, Hu B, et al. (2021): Development and validation of a prognostic gene signature correlated with M2 macrophage infiltration in esophageal squamous cell carcinoma. Front. Oncol. **11,** 769727 https://doi.org/10.3389/fonc.2021.769727
Yao Y (2017): Laminin: loss-of-function studies. Cell. Mol. Life Sci. **74,** 1095-1115 https://doi.org/10.1007/s00018-016-2381-0
Zeng W, Long X, Liu PS, Xie X (2023): The interplay of oncogenic signaling, oxidative stress and ferroptosis in cancer. Int. J. Cancer **153,** 918-931 https://doi.org/10.1002/ijc.34486

Received: April 25, 2025
Final version accepted: June 7, 2025

doi: 10.4149/gpb_2025029

Supplementary Material

Transcription factor SPI1 exacerbates the malignant progression of esophageal squamous cell carcinoma byactivating LAMA3 expression

Juan Qin[1,*], Yunxiang Tang[2,*], Rui Zhu[3], Xuqin Feng[1], Jun Bie[1], Qikun Lv[4] and Yang Shu[5]

[1] *Department of Oncology, Beijing Anzhen Nanchong Hospital, Capital Medical University & Nanchong Central Hospital, Nanchong, Sichuan, China*
[2] *Department of Nuclear Medicine, Chongging University Central Hospital, Chongging Emergency Medical Center, Chongqing, China*
[3] *Department of Intensive Care Unit, Beijing Anzhen Nanchong Hospital, Capital Medical University & Nanchong Central Hospital, Nanchong, Sichuan, China*
[4] *Chongqing Key Laboratory of Translational Research for Cancer Metastasis and Individualized Treatment, Chongqing University Cancer Hospital & Chongqing Cancer Institute & Chongqing Cancer Hospital, Chongqing, China*
[5] *Department of Obstetrics and Gynecology, The Second Affiliated Hospital of Chongqing Medical University, Chongqing, China*

Supplementary Figure

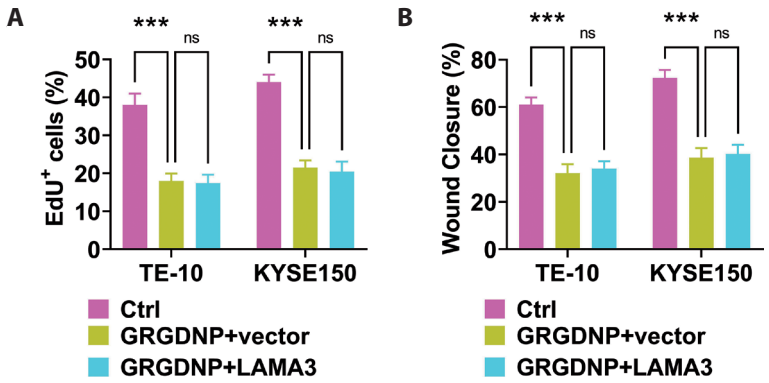

Figure S1. Effect of GRGDNP on the tumor-promoting effects of LAMA3. TE-10 and KYSE150 cells were divided into three groups: the Ctrl group, GRGDNP+vector group, and GRGDNP+LAMA3 group. **A.** Cell proliferation was evaluated by EdU assay. **B.** Cell migration was examined using wound healing assay. Differences in data were assessed by one-way ANOVA. *** $p < 0.001$.